Unfractionated heparin potently inhibits the binding of SARS-CoV-2 spike protein to a human cell line

Lynda J. Partridge[1], Luke R. Green[2]*, Peter N. Monk[2]

[1]Department of Molecular Biology and Biotechnology, The University of Sheffield, Sheffield, UK

[2]Department of Infection, Immunity and Cardiovascular Disease, The University of Sheffield, Sheffield, UK

* Corresponding author

E-mail: l.r.green@sheffield.ac.uk (LRG)

Abstract

The SARS-CoV-2 spike protein is known to bind to the receptor, ACE2, on the surface of target cells. The spike protein is processed by membrane proteases, including TMPRSS2, and is either internalised or fuses directly with the cell, leading to infection. We identified a human cell line that expresses both ACE2 and TMPRSS2, the RT4 urinary bladder transitional carcinoma, and used it to develop a proxy assay for viral interactions with host cells. A tagged recombinant form of the spike protein, containing both the S1 and S2 domains, binds strongly to RT4 cells as determined by flow cytometry. Binding is temperature dependent and increases sharply at 37°C, suggesting that processing of the spike protein is likely to be important in the interaction. As the spike protein has previously been shown to bind heparin, a soluble glycosaminoglycan, we used a flow cytometry assay to determine the effect of heparin on spike protein binding to RT4 cells. Unfractionated heparin inhibited spike protein binding with an IC_{50} value of <0.05U/ml whereas two low molecular weight heparins were much less effective. This suggests that heparin, particularly unfractionated forms, could be considered to reduce clinical manifestations of COVID-19 by inhibiting continuing viral infection. Despite the sensitivity to heparin, we found no evidence that host cell glycosaminoglycans such as heparan and chondroitin sulphates play a major role in spike protein attachment.

Introduction

SARS-CoV-2, the causative agent of COVID-19, is thought to infect cells after binding with high affinity to a host cell receptor, ACE2 (1). The ACE2 binding domain is located in the spike protein that consists of two domains: S1, which has a high affinity receptor binding domain (RBD) and S2, which contains sequences necessary for fusion with the host cell. S1 and S2 are linked by a sequence that contains a putative furin cleavage site that is critical for the entry of the virus into human cells (2). A cell-surface host serine protease, TMPRSS2, is also thought to be involved in viral entry and is proposed to cleave S1 and S2, leading to activation of the fusion machinery (1). By analogy with SARS-CoV, it is expected that the virus can fuse at the cell surface or later, following internalisation (reviewed in (3)).

Paradoxically, ACE2 is expressed at quite low levels by most cell types (e.g. (4)) and by very few cell lines leading to suggestions that additional receptor sites must exist. Viruses, such as herpes simplex and the β coronavirus family are known to interact with host glycosaminoglycans (5). A growing body of evidence suggests that SARS-CoV-2 can bind the glycosaminoglycans, heparan sulphate and heparin, dependent on their level of sulphation (preprints (6-8)) and that heparin can inhibit SARS CoV 2 entry in to Vero cells. Initial binding to heparan sulphates is thought to keep the spike protein within an ‘open’ conformation allowing for downstream binding and processing of ACE2 and TMPRSS2 respectively (7).

Here we present a new assay for viral attachment to host cells, using a human bladder epithelial cell line that expresses both ACE2 and TMPRSS2. The intact viral spike protein, but not the isolated S1 domain, exhibit a temperature dependent binding activity that allows rapid detection by flow cytometry. We have used this

assay to confirm that heparin can inhibit viral infection but that heparan sulphates alone might not constitute an additional viral attachment mechanism.

Materials and Methods

Materials

Surfen, a glycosaminoglycan antagonist (S6951-5mg, Sigma) was stored as a 5mM solution in DMSO. Unfractionated heparin (Leo, 1000U/ml), dalteparin (25000IU/ml) and enoxaparin (10000IU/ml) were obtained from the Royal Hallamshire Hospital Pharmacy, Sheffield, UK.

Cell culture

The RT4 cell line was obtained from (ATCC® HTB-2™, American Tissue Type Collection) and routinely cultured in McCoys 5A medium (Thermo Fisher Scientific) supplemented with 10% foetal calf serum. The A549 cell line was obtained from the European Collection of Animal Cell Cultures (ECACC) and routinely cultured in DMEM supplemented with 10% foetal calf serum. Both cell lines were routinely sub-cultured by trypsinisation and maintained in sub-confluent cultures. For heparinase and chondroitinase treatment, RT4 cells were plated at $1x10^4$/well in 6 well plates overnight, washed once in Hanks' Balanced Salt Solution (HBSS) containing divalent cations and then incubated for 3 hr with 0.5U/ml heparinase I/III (Merck) or 0.25U/ml chondroitinase (Merck) diluted in McCoys 5A medium without serum. After washing with HBSS, the cells were harvested by brief trypsinisation and used in the spike protein binding assay.

Spike protein binding assay

Cells were harvested by brief trypsinisation and added to wells of a 96-well U bottom plate. After centrifugation at 300xg for 3 min and washing with HBSS containing divalent cations and 0.1% bovine serum albumin (BSA) (assay buffer, AB), cells were incubated with potential inhibitors in 50µl AB for 30 min at 37°C. The supernatant was removed following centrifugation and 25µl of AB containing S1-Fc (Stratech UK) or S1S2-His6 protein (Stratech UK) added before incubation at 4, 21 or 37°C for 60 min. Cells were washed once and then incubated with the appropriate fluorescently labelled secondary antibody (anti-mouse Ig-FITC, Sigma; or anti-His6 HIS.H8 DyLight 488, Invitrogen) for 30 min at 21°C. Cells were finally resuspended in 50µl AB containing propidium iodide and cell-associated fluorescence measured using a Guava 2L-6HT flow cytometer. Live cells were gated as a propidium iodide negative population and the median fluorescence (MFI) recorded. MFI was calculated after subtraction of cell-associated fluorescence of the secondary antibody alone. Where stated, the data were normalised to the untreated control cells.

Determination of spike protein binding to ACE2 by ELISA

ELISA plate wells (Maxisorb, Nunc) were coated with 1µg/ml recombinant human ACE2 (Biotechne) in coating buffer (0.05M sodium bicarbonate buffer, pH 9.6) overnight at 4°C. Following removal of excess ACE2, wells were washed twice with PBS 0.05% Tween, blocked with PBS 0.05% Tween 0.2% BSA for 2 hr at 37 °C and washed three times as previously. Various concentration of His-tagged spike proteins in blocking buffer (or blocking buffer control) were added to the wells (50µl/well) and incubated at 37 °C for 2 hr. Wells were washed three times as above then incubated at room temperature with 50µl/well biotin-labelled rabbit monoclonal

anti-His6 (Thermo Fisher Scientific) diluted to 1/1000 in blocking buffer for 1 hr, washed 3 times and incubated for 30 min with 50µl/well streptavidin-HRP (Pierce) diluted 1/200 in blocking buffer. After washing 3 times with PBS 0.05% Tween and twice with dH_2O, 50µl per well TMB substrate solution (Novex) was added followed by 50µl 1M HCl to quench the reaction. Absorbance was measured at OD_{450nm}.

Results

Selection of a cell line for viral attachment studies

The Protein Atlas database has information on mRNA expression in a wide variety of human cell lines (https://www.proteinatlas.org; (9)). Although HaCaT skin keratinocytes have the highest ACE2 expression, they do not express TMPRSS2 (Table 1). The Caco2 colorectal adenocarcinoma cell line expresses no ACE2 mRNA but quite high levels of TMPRSS2; this cell line has been used in several infection studies of SARS-CoV and SARS-CoV-2 (10). The urinary bladder epithelial transitional-cell carcinoma cell line RT4 (11), expresses low levels of ACE2 but very high levels of TMPRSS2, making this cell line a suitable choice for the study of viral attachment. Of note, RT4 also expresses ADAM17, a metalloprotease known to be involved in the processing of ACE2, and CD9, an adaptor protein that controls ADAM17 trafficking and activity. Finally, RT4 cells also express rhomboid-like 2, a protease known to associate with ADAM17. In contrast, the human lung adenocarcinoma alveolar basal epithelial cell line A549 expresses neither ACE2 or TMPRSS2, perhaps explaining why this cell line does not support infection by SARS-CoV-2 (12).

Table 1. Normalised mRNA expression values for ACE2 and potentially associated membrane proteins in several cell lines.

	RT4	A549	Caco2	HaCaT
ACE2	2.40	0.00	0.00	4.10
TMPRSS2	35.2	0.00	14.6	0.00
ADAM17	12.9	12.7	11.2	14.2
RHBDL2	6.00	18.8	5.50	13.9
CD9	94.7	14.9	10.9	74.5

Normalised mRNA expression values are provided from the Protein Atlas database (https://www.proteinatlas.org).

Expression of ACE2 and ADAM17 at the surface of RT4 cells

We used flow cytometry to determine the expression of several membrane proteins on RT4 and A549 cells. ACE2 was detected only on the surface of RT4 cells, whereas both cell lines expressed ADAM17 (Fig 1).

Figure 1. Expression of ACE2 on the surface of RT4 but not A549 cells. RT4 and A549 cells were stained with goat anti-human ACE2 or mouse anti-human ADAM17 antibodies and the appropriate fluorescent secondary antibodies. Panel A shows the histograms for RT4 and A549 surface ACE2 and ADAM 17 expression (black line) and the secondary-antibody only control (grey). Panel B shows the relative expression on the two cells lines. MFI was calculated as a percentage of the secondary antibody-only controls.

Binding of SARS-CoV-2 spike proteins to RT4 and A549 cells

To detect spike protein binding, we used recombinant S1 and S1S2, tagged with mouse Fc and His6, respectively. Following published binding studies for S1 (13), binding was performed initially at 21°C, using fluorescently labelled secondary anti-tag antibodies to stain cells for flow cytometry. Only a very low level of S1 binding to RT4 cells was detected, and S1 binding to A549 cells was undetectable (S1 Fig). In contrast, S1S2 protein bound strongly to subsets of both RT4 and A549 cells, with a higher percentage of RT4 cells positive when compared to A549 cells (Fig 2A). Binding was detectable from 100nM S1S2 (Fig 2B) but was not saturated at 330nM, the highest concentration that could be used due to limited availability of the S1S2 protein.

Figure 2. Recombinant S1S2 SARS-CoV-2 spike protein binds to RT4 and A549 cells at 21°C. RT4 cells were incubated with His6-tagged S1S2 protein for 30 min at 21°C and then with anti-His6 secondary antibody labelled with Dylight 488. Cell associated fluorescence was measured by flow cytometry. Panel A shows 330nM S1S2 binding (red line) compared to secondary-only control (grey). The histograms are representative of two separate experiments conducted in duplicate. Panel B shows binding to RT4 cells measured as the number of cells more positive than the secondary antibody alone expressed as a percentage of the secondary-only controls (NA) for S1S2 from a single experiment conducted in duplicate.

To determine if the levels of detectable S1S2 binding to RT4 cells were being affected by internalisation of the tagged protein, we performed binding experiments at both 4°C, which should largely inhibit internalisation, and at 37°C, which should be

166 permissive for internalisation. Surprisingly, the binding of S1S2 at 37°C was much
167 stronger than at 4°C or 21°C (Fig 3), with all cells stained. In contrast, S1 protein
168 binding was undetectable at 4°C and only slightly elevated at 37°C (Fig 3). We were
169 unable to determine the affinity of the interaction due to a limited availability of
170 recombinant S1S2, but binding was still increasing even at 330nM (Fig 4A),
171 suggesting a relatively low affinity interaction. This is in contrast to published reports
172 of the affinity of S1 for HEK cells overexpressing human ACE2 (~10nM) (13). Binding
173 to A549 cells at 37°C was much lower than to RT4 cells (Fig 4A, B) at all
174 concentrations tested although the cytometry histogram indicated that all cells could
175 bind some S1S2. This suggests that the binding at 37°C may be at least partly
176 dependent on ACE2 and/or TMPRSS2 expression. S1S2 must be internalised only
177 slowly, if at all, over the time course of the assay at 37°C. However, the temperature
178 dependency suggests that S1S2 might undergo a conformational change, perhaps
179 as a result of proteolytic processing at the cell surface.

180

181 **Figure 3. S1S2 binding to RT4 cells dramatically increases at 37°C.** RT4 cells
182 were incubated with 330nM S1-Fc (A, C) or 330nM S1S2-His6 protein (C, D) for 60
183 min at either 4°C (A, B) or 37°C (C, D), before staining with anti-mouse Ig labelled
184 with FITC or anti-His6 secondary antibody labelled with Dylight 488 for 30 min at
185 21°C. Cell-associated fluorescence was measured using flow cytometry. Grey shows
186 secondary-only control.

187 **Figure 4. WT S1S2 binds more strongly to RT4 than to A549 cells.** Panel A
188 shows a dose-response curve for S1S2 binding to RT4 and A549 cells at 37°C, for
189 S1S2. The data are the means from a single experiment conducted in duplicate.

Panel B shows representative histograms of 100nM S1S2 binding to RT4 and A549 cells at 37°C (black lines), compared to secondary antibody alone (grey).

Unfractionated heparin inhibits S1S2 binding to RT4 cells

Having developed a novel assay that should mimic some aspects of SARS-CoV-2 infection, we used it to test potential inhibitors. Heparin has been reported to bind directly to S1 and to interfere with SARS-CoV-2 infection (8) and so we tested the effects of pre-incubating RT4 cells with heparin on the S1S2 binding at 37°C. Unfractionated heparin (UFH) at 10U/ml inhibited 80% of 330nM S1S2 binding to the cells (Fig 5A) and reached significance compared to untreated controls (Fig 5B). Using 100nM S1S2, the inhibition by UFH was complete with an IC_{50} of 0.033U/ml (95% confidence interval 0.016-0.07) (Fig 6). This is far below the target prophylactic and therapeutic concentrations in serum, 0.1-0.4U/ml and 0.3-0.7U/ml, respectively (14, 15). In contrast, two low molecular weight heparins, dalteparin and enoxaparin, were both only partial inhibitors, and were less potent than UFH (IC_{50} values of 0.558 and 0.072IU/ml, respectively). Typical prophylactic and therapeutic serum concentrations of LMWH are 0.2-0.5IU/ml 0.5-1.2IU/ml (16), suggesting that dalteparin may be used below the effective dose required for inhibition of viral infection if used prophylactically.

Figure 5. Unfractionated heparin inhibits S1S2 binding to RT4 cells. RT4 cells were pre-treated with 10U/ml unfractionated heparin for 30 min at 37°C before the addition of 330nM S1S2. After a further 60 min at 37°C, cells were washed and

fluorescent secondary anti-His6 added for a further 30 min at 21°C. Cell-associated fluorescence was measured by flow cytometry. Panel A shows a representative histogram with S1S2 binding (blue line), S1S2 binding after heparin treatment (black line) and secondary antibody only (grey). Panel B shows the effects of 10U/ml heparin pre-treatment on 330nM S2S2 binding, as a percentage of the S1S2 binding to untreated (NA) control cells. Data are from four separate experiments in duplicate ±SEM. Significance to NA, ** $p<0.01$, one sample t test.

Figure 6. Concentration dependent inhibition of S1S2 binding by unfractionated heparin and low molecular weight heparins, dalteparin and enoxaparin. RT4 cells were pre-incubated with the stated concentrations of unfractionated heparin, enoxaparin and dalteparin for 30 min at 37°C, then with 100nM S1S2 for a further 60 min at 37°C. After a further 60 min at 37°C, cells were washed and fluorescent secondary anti-His6 added for a further 30 min at 21°C. Cell-associated fluorescence was measured by flow cytometry and are shown as a percentage of the S1S2 binding to untreated control cells. Data are the means ± SD of 2-3 experiments performed in duplicate.

The inhibitory activity of heparin is specific to S1S2 binding to cells

ACE2 binding by both S1 and S1S2 proteins was detected in ELISA using immobilised ACE2, with EC_{50} values of ~20nM (S2 Fig A), similar to published data (13). The presence of 10U/ml UFH did not interfere with the recognition of ACE2 (S2 Fig B). The effect of UFH was also not caused by blockade of the His6 tag-antibody interaction (S3 Fig C), which was not affected in ELISA by concentrations of UFH of 500U/ml.

No evidence for S1S2 binding to heparan sulphates on RT4 cells

An interaction with heparin suggests that S1S2 protein may also interact with heparan sulphate glycosaminoglycans at the host cell surface, as has previously been shown for SARS-CoV-1 (17) and more recently with SARS-CoV-2 (7). RT4 cells were treated for 3 hours with 0.5U/ml of a heparanase I and III blend, or 0.25U/ml chondroitinase before S1S2 binding was tested. Neither treatment resulted in a significant reduction in S1S2 binding (Fig 7A). Surfen, a glycosaminoglycan antagonist, has been shown to completely inhibit FGF2 binding to heparan sulphates on CHO cells at concentrations between 5-20µM (18). Treatment of RT4 cells with 16.5µM-0.45µM surfen, resulted in only a ~40% reduction in S1S2 binding (Fig 7B). These data suggest that heparan sulphates play only a minor role in spike protein attachment to host cells.

Figure 7. Removal or blockade of heparan sulphates has only minor effects on S1S2 binding. RT4 cells were pre-treated with heparinase I/III or chondroitinase (Panel A) for 3 hrs or surfen for 30 min (Panel B) at 37°C before incubation with 100nM S1S2 for a further 60 min at 37°C. After a further 60 min at 37°C, cells were washed and fluorescent secondary anti-His6 added for a further 30 min at 21°C. Cell-associated fluorescence was measured by flow cytometry and are shown as a percentage of the S1S2 binding to untreated control cells. Panel A, data are the means ± SD from two separate experiments performed in duplicate. Panel B, data are the means ± SD of four separate experiments conducted in duplicate.

Discussion

We have demonstrated that intact recombinant S1S2 spike protein but not the S1 domain from SARS-CoV-2 can bind strongly to a human cell line that expresses ACE2 and TMPRSS2. We have developed this as an assay to test potential inhibitors of viral infection and shown that UFH and two low molecular weight heparins (LMWH) in use clinically can inhibit S1S2 binding. The same activity profile for UFH and one LMWH (enoxaparin) has been demonstrated in SARS-CoV-2 infection of Vero cells (8). These authors also showed that heparin could interact with recombinant S1 RBD and cause conformational changes, leading to the suggestion that SARS-CoV-2 might use host heparan sulphates as an additional attachment site during infection. Although our data supports the inhibitory activity of UFH, it does not support the conjecture that heparan sulphates are essential for viral infection. Studies have also suggested the importance of differing glycan sulphation states in different tissues as an explanation for viral tropism. Recently, SARS-CoV-2 spike protein S1 has been shown to bind heparan sulphates with varying degrees of sulphation with differing affinities; chain length and 6-O-sulphation were particularly important (7). Furthermore, heparin could also be inhibiting host proteases that are necessary to process the spike protein, as previously hypothesised (19).

LMWH are smaller (<8kDa) than UFH, which is a mix of polysaccharide chain lengths from ~5-40kDa, and have more predictable pharmacokinetics (20). LMWH are commonly used both prophylactically and therapeutically in COVID-19 patients and have been reported to improve patient outcome (21)). Our work and the work of Mycroft-West et al (8) suggests that thought be given to the earlier use of heparin when viral infection is still an important driver of disease severity. The use of UFH

rather than LMWH should also be considered, although we note that administration and the safety profile of UFH might preclude this in some cases (22).

In conclusion, we have developed a simple flow cytometric assay for SARS-CoV-2 spike protein binding to human cells, confirming an earlier finding concerning inhibition of whole live virus binding to African green monkey cells using heparin. Our new assay could be a useful first screen for novel inhibitors of coronavirus infection.

Acknowledgements

The authors would like to Dr Stephane Mesnage for flow cytometry and the staff of the Molecular Biology and Biotechnology Department for access to laboratory space.

References

1. Hoffmann M, Kleine-Weber H, Schroeder S, Kruger N, Herrler T, Erichsen S, et al. SARS-CoV-2 Cell Entry Depends on ACE2 and TMPRSS2 and Is Blocked by a Clinically Proven Protease Inhibitor. Cell. 2020;181(2):271-80 e8.

2. Hoffmann M, Kleine-Weber H, Pohlmann S. A Multibasic Cleavage Site in the Spike Protein of SARS-CoV-2 Is Essential for Infection of Human Lung Cells. Mol Cell. 2020.

3. Hofmann H, Pohlmann S. Cellular entry of the SARS coronavirus. Trends Microbiol. 2004;12(10):466-72.

4. Li MY, Li L, Zhang Y, Wang XS. Expression of the SARS-CoV-2 cell receptor gene ACE2 in a wide variety of human tissues. Infect Dis Poverty. 2020;9(1):45.

5. O'Donnell CD, Shukla D. The Importance of Heparan Sulfate in Herpesvirus Infection. Virol Sin. 2008;23(6):383-93.

6. Liu L, Chopra P, Li X, Wolfert M, Tompkins MS, Boons G-J. SARS-CoV-2 spike protein binds heparan sulfate in a length- and sequence-dependent manner. bioRxiv. 2020.

309 7. Hao W, Ma B, Li Z, Wang X, Gao X, Li Y, et al. Binding of the SARS-CoV-2 Spike
310 Protein to Glycans. BioRxiv. 2020.
311 8. Mycroft-West CJ, Su D, Pagani I, Rudd TR, Elli S, FGuimond SE, et al. Heparin
312 inhibits cellular invasion by SARS-CoV-2: structural dependence of the interaction of the
313 surface protein (spike) S1 receptor binding domain with heparin. BioRxiv. 2020.
314 9. Uhlen M, Zhang C, Lee S, Sjostedt E, Fagerberg L, Bidkhori G, et al. A pathology
315 atlas of the human cancer transcriptome. Science. 2017;357(6352).
316 10. Kim JM, Chung YS, Jo HJ, Lee NJ, Kim MS, Woo SH, et al. Identification of
317 Coronavirus Isolated from a Patient in Korea with COVID-19. Osong Public Health Res
318 Perspect. 2020;11(1):3-7.
319 11. O'Toole C, Perlmann P, Unsgaard B, Almgard LE, Johansson B, Moberger G, et al.
320 Cellular immunity to human urinary bladder carcinoma. II. EEffect of surgery and
321 preoperative irradiation. Int J Cancer. 1972;10(1):92-8.
322 12. Matsuyama S, Nao N, Shirato K, Kawase M, Saito S, Takayama I, et al. Enhanced
323 isolation of SARS-CoV-2 by TMPRSS2-expressing cells. Proc Natl Acad Sci U S A.
324 2020;117(13):7001-3.
325 13. Tai W, Zhang X, He Y, Jiang S, Du L. Identification of SARS-CoV RBD-targeting
326 monoclonal antibodies with cross-reactive or neutralizing activity against SARS-CoV-2.
327 Antiviral Res. 2020:104820.
328 14. Hirsh J, Warkentin TE, Shaughnessy SG, Anand SS, Halperin JL, Raschke R, et al.
329 Heparin and low-molecular-weight heparin: mechanisms of action, pharmacokinetics,
330 dosing, monitoring, efficacy, and safety. Chest. 2001;119(1 Suppl):64S-94S.
331 15. Lehman CM, Frank EL. Laboratory Monitoring of Heparin Therapy: Partial
332 Thromboplastin Time or Anti-Xa Assay? Labmedicine. 2009;40(1):47-51.
333 16. Weitz JI. Low-molecular-weight heparins. New Engl J Med. 1997;337(10):688-98.
334 17. Lang J, Yang N, Deng J, Liu K, Yang P, Zhang G, et al. Inhibition of SARS
335 pseudovirus cell entry by lactoferrin binding to heparan sulfate proteoglycans. PLoS One.
336 2011;6(8):e23710.

18. Schuksz M, Fuster MM, Brown JR, Crawford BE, Ditto DP, Lawrence R, et al. Surfen, a small molecule antagonist of heparan sulfate. Proc Natl Acad Sci U S A. 2008;105(35):13075-80.

19. Belen-Apak FB, Sarialioglu F. The old but new: Can unfractioned heparin and low molecular weight heparins inhibit proteolytic activation and cellular internalization of SARS-CoV2 by inhibition of host cell proteases? Med Hypotheses. 2020;142:109743.

20. Samama M, Bernard P, Bonnardot JP, Combe-Tamzali S, Lanson Y, Tissot E. Low molecular weight heparin compared with unfractionated heparin in prevention of postoperative thrombosis. Br J Surg. 1988;75(2):128-31.

21. Tang N, Bai H, Chen X, Gong J, Li D, Sun Z. Anticoagulant treatment is associated with decreased mortality in severe coronavirus disease 2019 patients with coagulopathy. J Thromb Haemost. 2020;18(5):1094-9.

22. Junqueira DR, Perini E, Penholati RR, Carvalho MG. Unfractionated heparin versus low molecular weight heparin for avoiding heparin-induced thrombocytopenia in postoperative patients. Cochrane Database Syst Rev. 2012(9):CD007557.

Supporting information

S1 Fig. S1-Fc binding to RT4 and A549 cells is very low. RT4 or A549 cells were incubated with 330nM mouse Fc-tagged S1S2 protein for 30 min at 21°C and then with anti-mouse Ig secondary antibody labelled with FITC. Cell associated fluorescence was measured by flow cytometry. The histograms show S1 binding (black line) compared to secondary-only control (grey) and are representative of several separate experiments conducted in duplicate.

S2 Fig. S1S2 binds to ACE2 in ELISA and binding is not inhibited by unfractionated heparin. In panels A and C, recombinant human ACE2 was

immobilised on an ELISA plate. For C, 10U/ml of unfractionated heparin was added for 30 min at 37°C. Recombinant human S1S2 was incubated at the stated concentrations (A) or at 65nM (C) for 2 hrs before the addition of biotinylated anti-His6 antibody (S1S2) or an anti-mouse Ig antibody labelled directly with horseradish peroxidase (S1). Bound S1S2 was visualised using streptavidin-horseradish peroxidase and developed using TMB. In panel B, two His6-tagged proteins (human C5a and SARS-CoV-2 S1 RBD) were immobilised on the plate before visualisation using streptavidin-horseradish peroxidase and developed using TMB. The absorbance was measured at 450nm. Data are the results of single experiments performed in duplicate (A, B) or in triplicate (C).

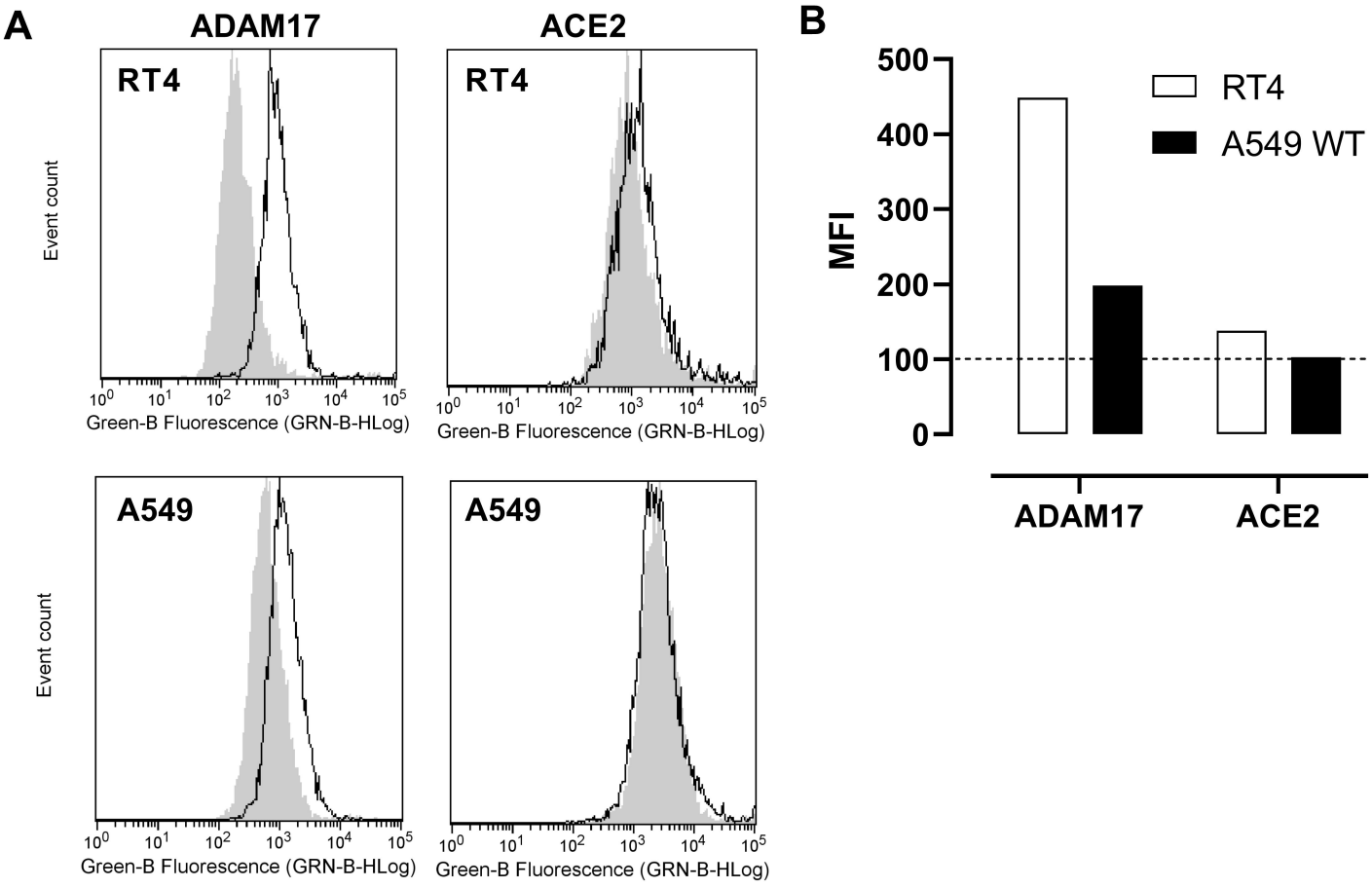
A
ADAM17
ACE2
RT4
RT4
Event count
Green-B Fluorescence (GRN-B-HLog)
Green-B Fluorescence (GRN-B-HLog)
A549
A549
Event count
Green-B Fluorescence (GRN-B-HLog)
Green-B Fluorescence (GRN-B-HLog)
B
MFI
500
400
300
200
100
0
RT4
A549 WT
ADAM17
ACE2

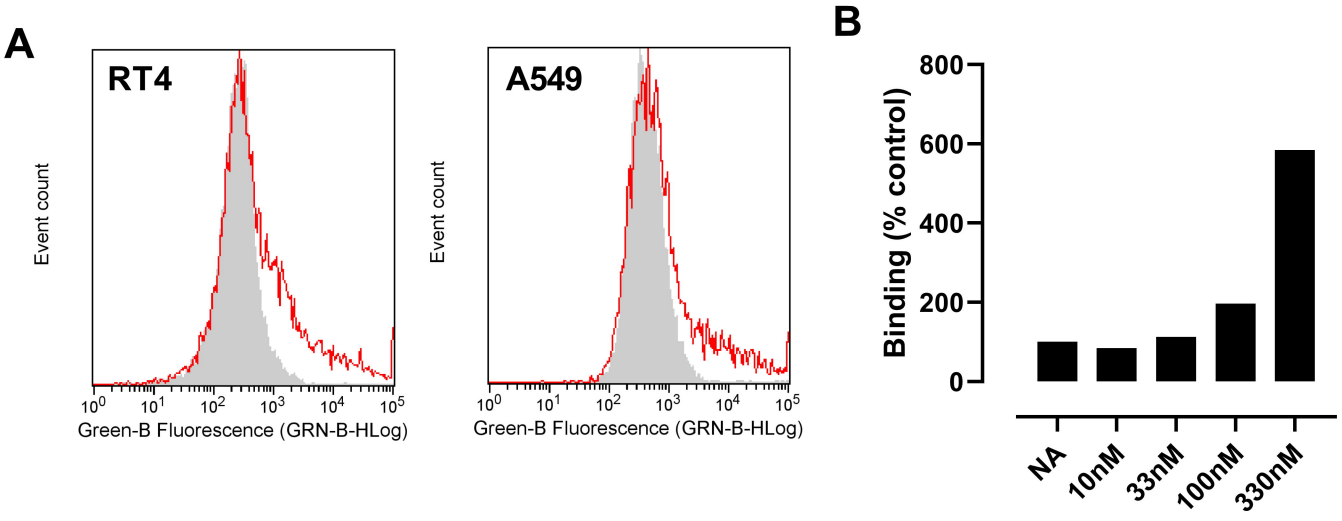
A
RT4
A549
Event count
Event count
Green-B Fluorescence (GRN-B-HLog)
Green-B Fluorescence (GRN-B-HLog)
B
Binding (% control)
800
600
400
200
0
NA
10nM
33nM
100nM
330nM

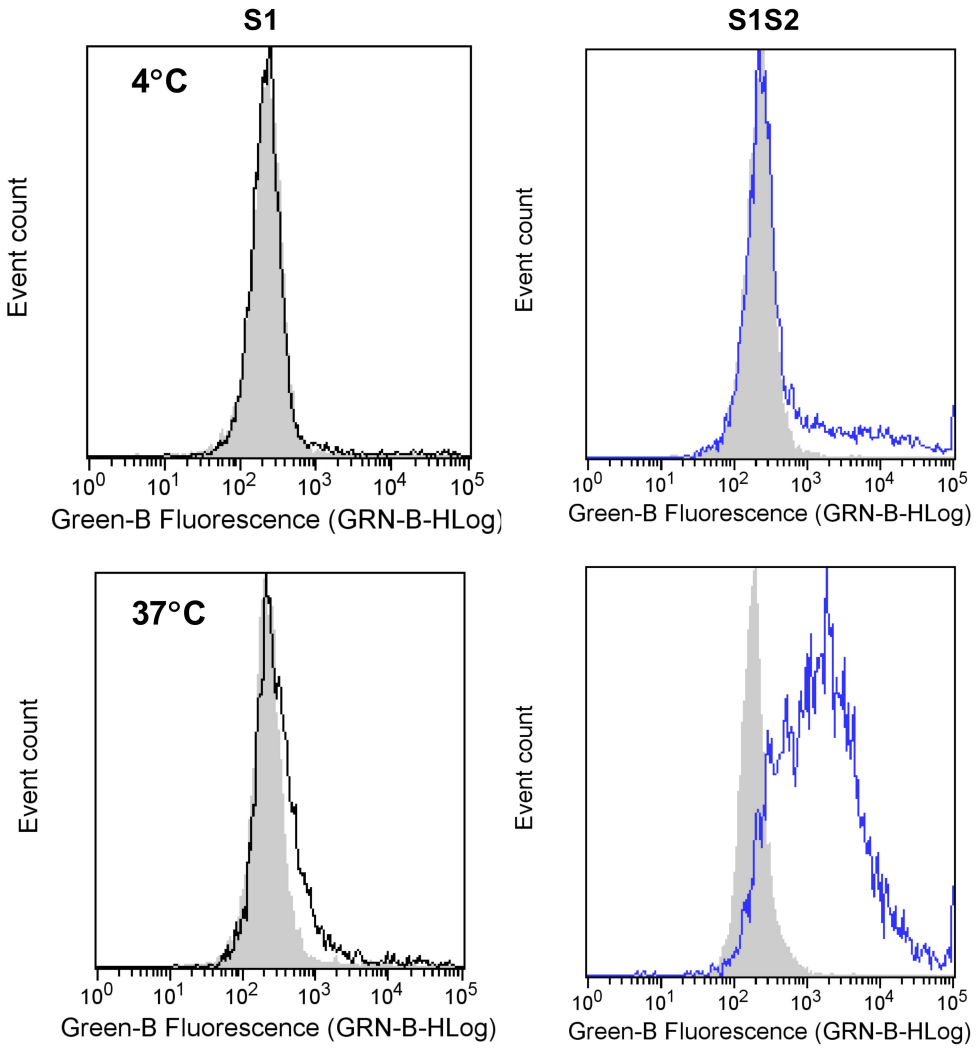
S1
S1S2
4°C
37°C
Event count
Green-B Fluorescence (GRN-B-HLog)
10^0 10^1 10^2 10^3 10^4 10^5

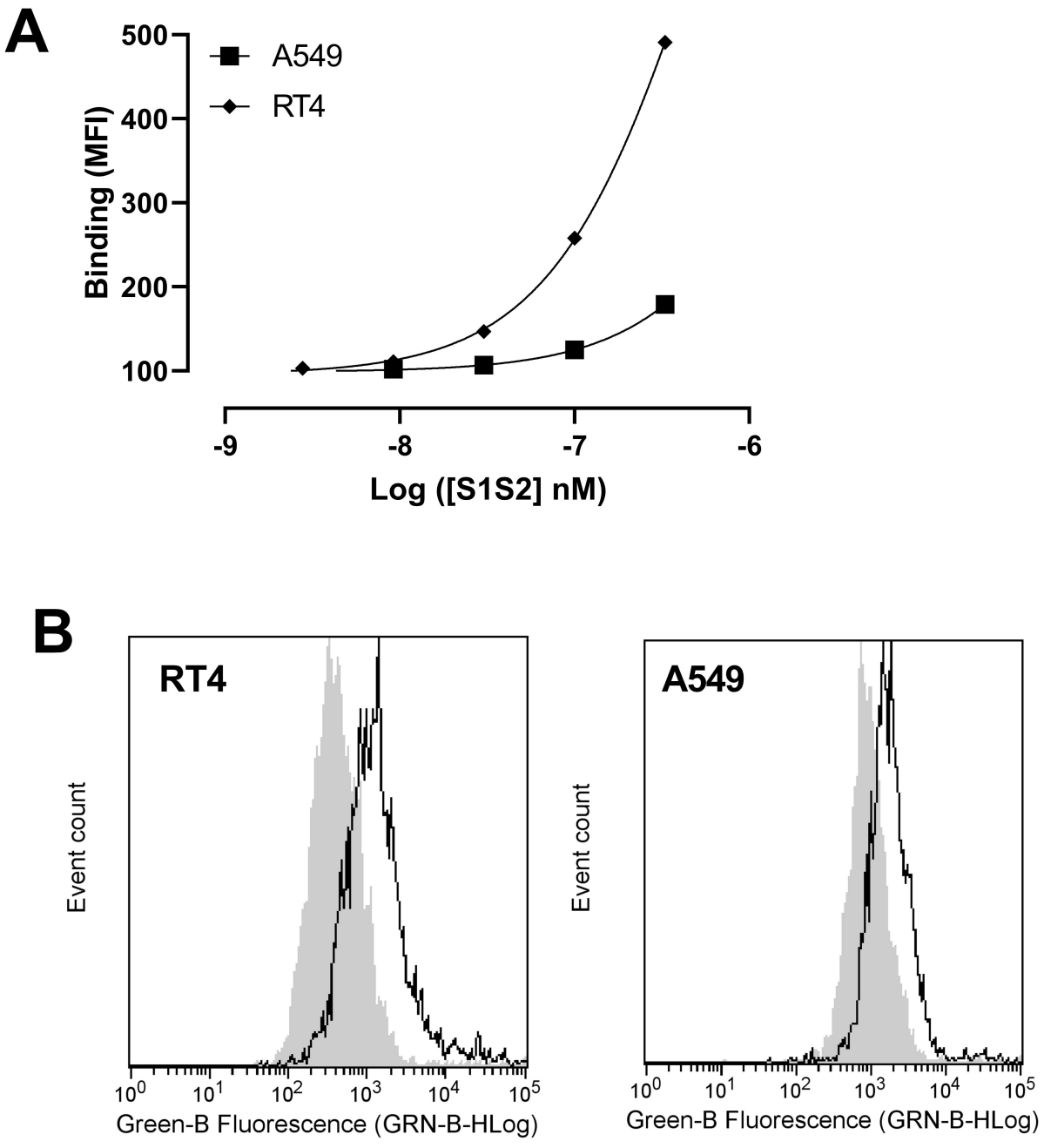
A
500
400
300
200
100
Binding (MFI)
A549
RT4
-9
-8
-7
-6
Log ([S1S2] nM)
B
RT4
Event count
10^0 10^1 10^2 10^3 10^4 10^5
Green-B Fluorescence (GRN-B-HLog)
A549
Event count
10^0 10^1 10^2 10^3 10^4 10^5
Green-B Fluorescence (GRN-B-HLog)

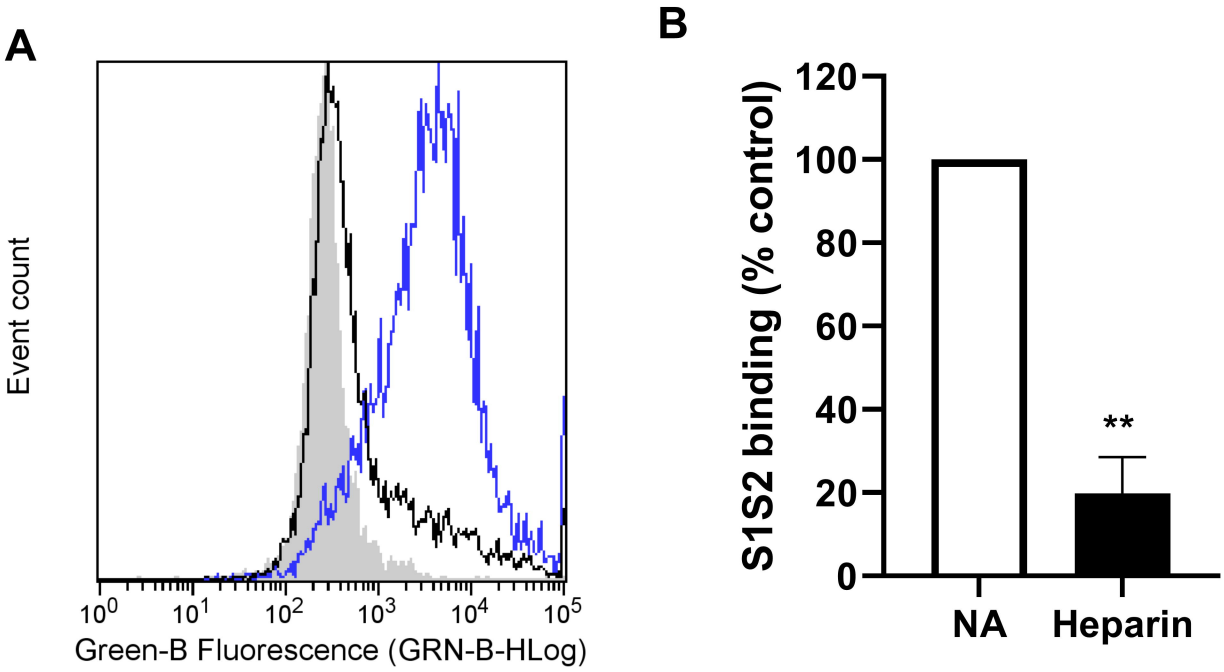
A
Event count
10^0
10^1
10^2
10^3
10^4
10^5
Green-B Fluorescence (GRN-B-HLog)
B
S1S2 binding (% control)
120
100
80
60
40
20
0
**
NA
Heparin

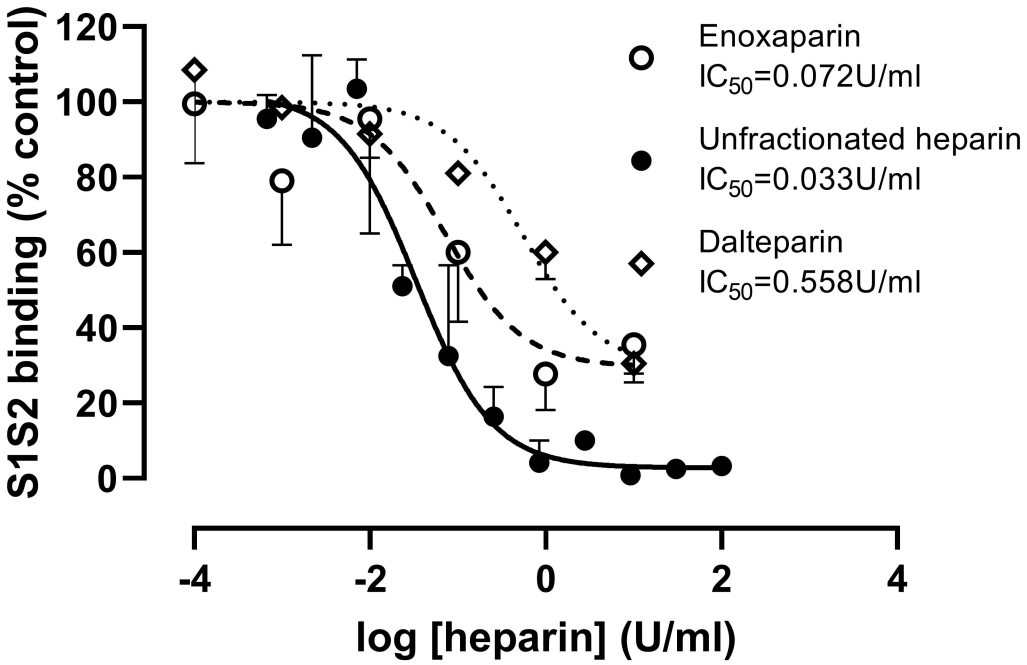
S1S2 binding (% control)
120
100
80
60
40
20
0
-4
-2
0
2
4
log [heparin] (U/ml)
Enoxaparin
IC50=0.072U/ml
Unfractionated heparin
IC50=0.033U/ml
Dalteparin
IC50=0.558U/ml

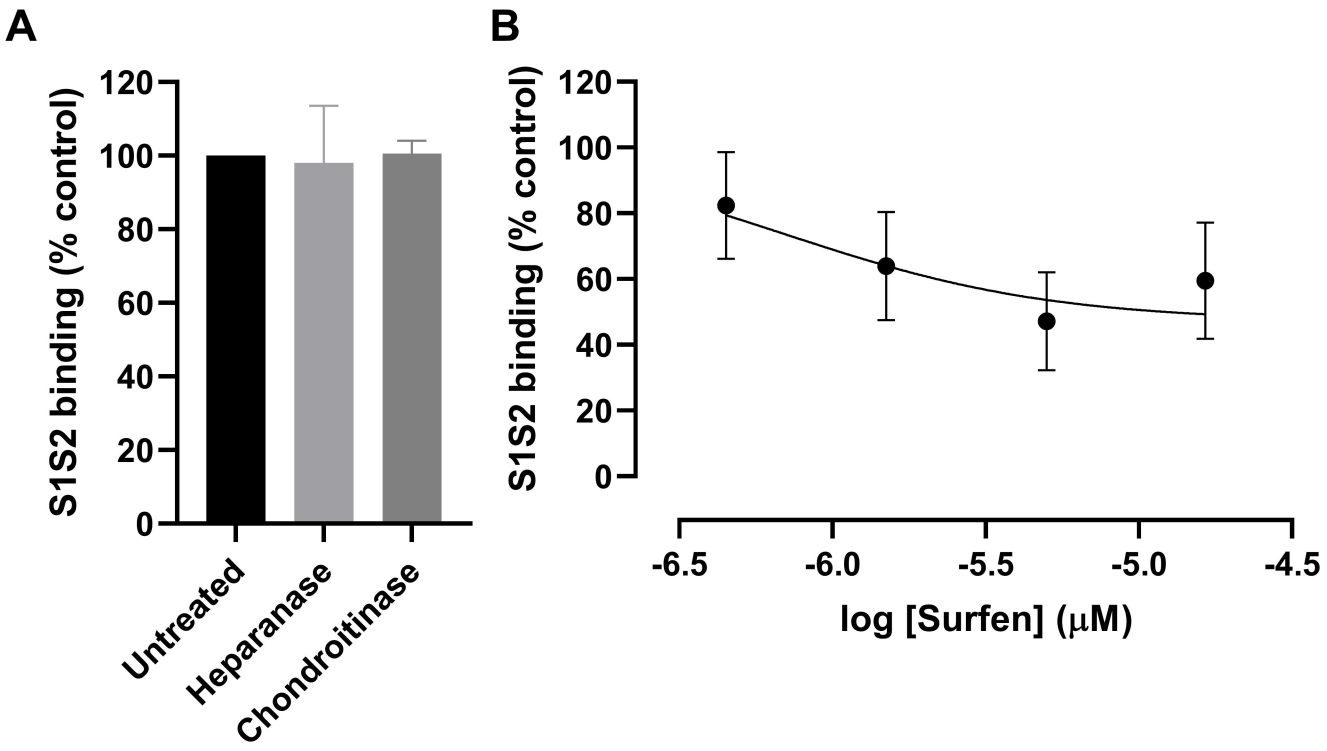
A
S1S2 binding (% control)
120
100
80
60
40
20
0
Untreated
Heparanase
Chondroitinase
B
S1S2 binding (% control)
120
100
80
60
40
20
0
-6.5
-6.0
-5.5
-5.0
-4.5
log [Surfen] (μM)